

Supporting Information

Surface plasmon resonance as a breakthrough tool for characterizing the size and shape of graphene quantum dots

Giuseppe Stefano Basile, Damiano Calcagno, Nunzio Tuccitto, Benoit Maxit, Pascal Boulet, Mélanie Emo, Liang Liu, Giuseppe Grasso * and Philippe Pierrat *

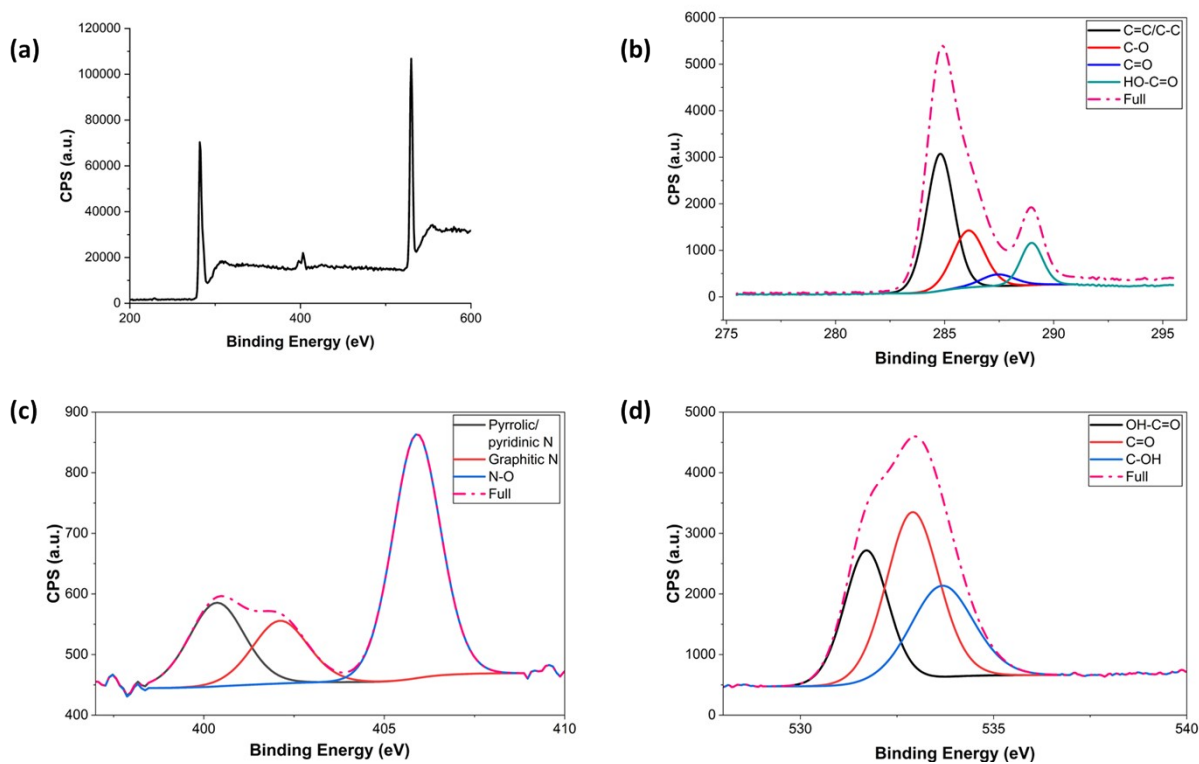


Fig. S1. XPS spectra of GQDs-01: (a) survey spectrum, (b) high-resolution C1S spectrum, (c) high-resolution N1S spectrum and (d) high-resolution O1S spectrum.

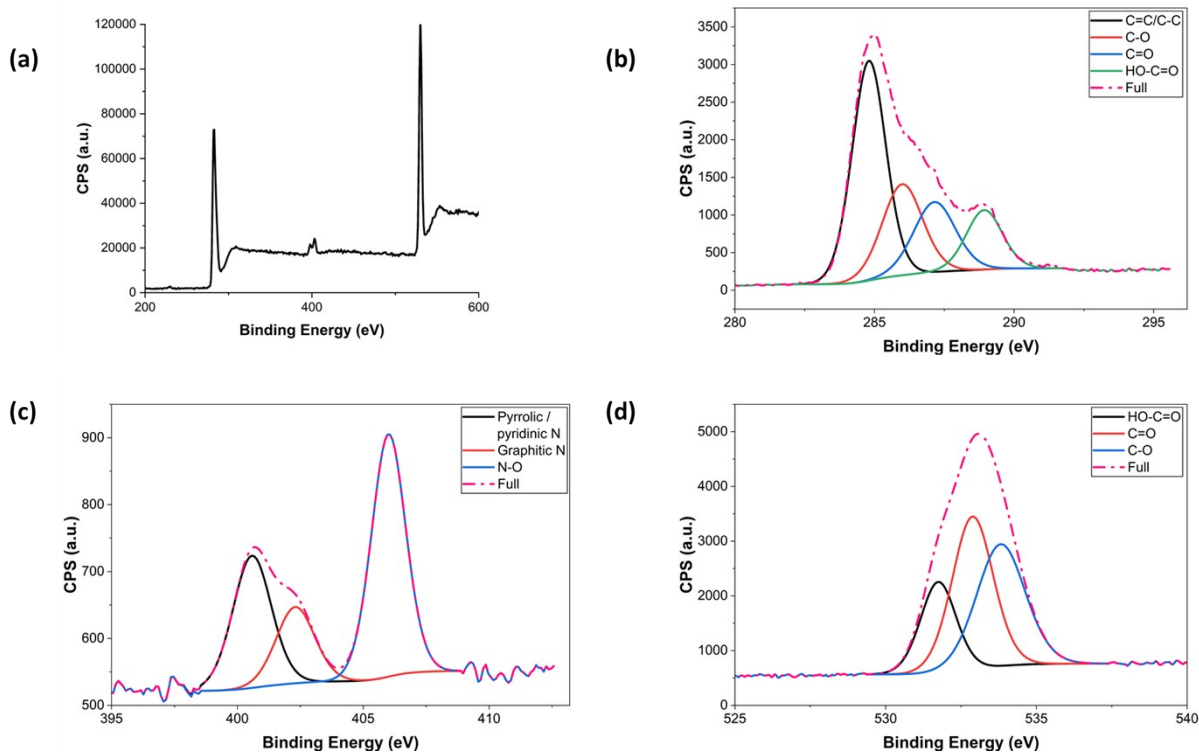


Fig. S2. XPS spectra of GQDs-02: (a) survey spectrum, (b) high-resolution C1s spectrum, (c) high-resolution N1s spectrum and (d) high-resolution O1s spectrum.

Table S1. Elemental composition obtained from the XPS wide spectra

| | Elemental composition | | |
|----------------|-----------------------|------|-----|
| | C1s | O1s | N1s |
| GQDs-01 | 65,0 | 29,2 | 5,1 |
| GQDs-02 | 66,2 | 28,2 | 5,0 |

Table S2. Carbon bond composition obtained using the high resolution XPS C1s spectra

| | Carbon bond composition (C1s, %) | | | |
|----------------|----------------------------------|------|------|--------|
| | C=C / C-C | C-O | C=O | HO-C=O |
| GQDs-01 | 54,6 | 26,1 | 5,7 | 13,6 |
| GQDs-02 | 45,9 | 22,7 | 18,1 | 13,2 |

Table S3. Oxygen bond composition obtained using the high resolution XPS O1s spectra

| | Carbon bond composition (O1s, %) | | |
|----------------|----------------------------------|------|------|
| | HO-C=O | C=O | C-OH |
| GQDs-01 | 28,8 | 43,2 | 28,0 |
| GQDs-02 | 21 | 40,6 | 38,4 |

Table S4. Nitrogen bond composition obtained using the high resolution XPS N1s spectra

| | Carbon bond composition (N1s, %) | | |
|----------------|----------------------------------|-------------|------|
| | Pyrrolic / Pyrrolic N | Graphitic N | N-O |
| GQDs-01 | 23,5 | 17,6 | 58,9 |
| GQDs-02 | 31,2 | 18,0 | 50,8 |

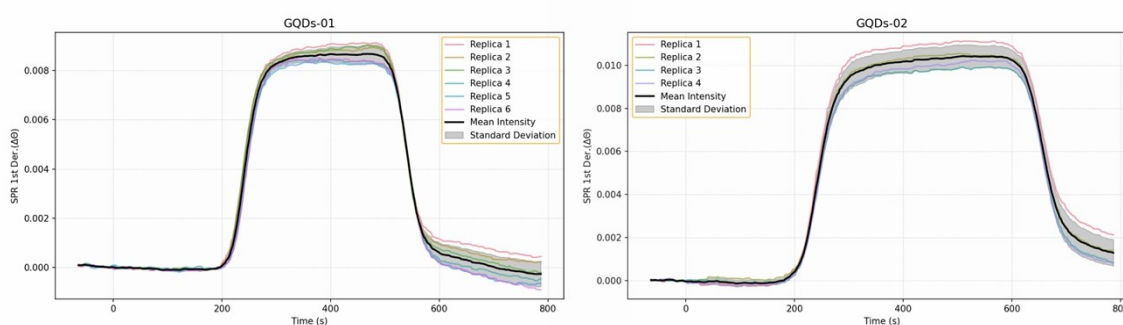


Fig. S3. Surface Plasmon Resonance raw sensograms of GQDs-01 (left) and GQDs-02 (right) samples. Multicolor lines represent the experimental replicas; the black line is the mean curve, while the grey shadow depicts the standard deviation.

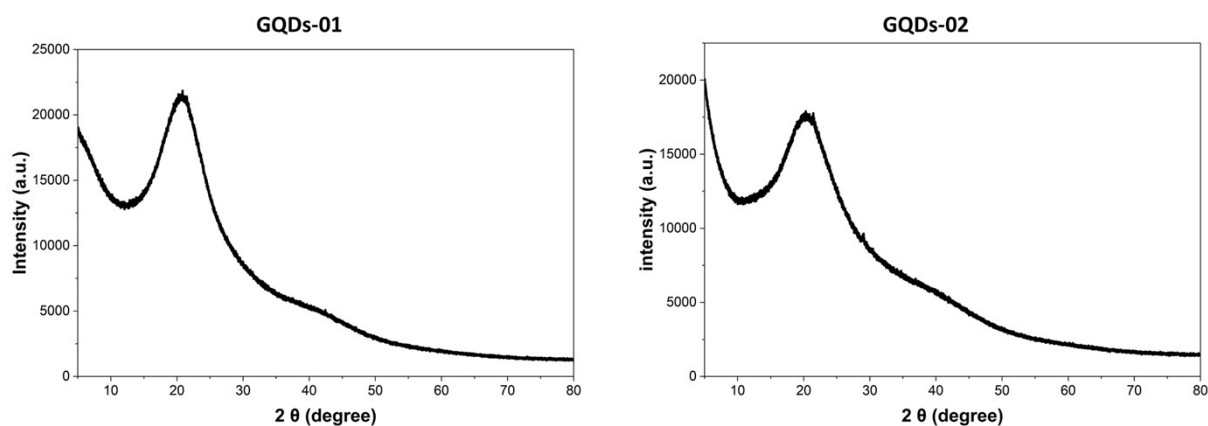


Fig. S4. XRD pattern of GQDs-01 (left) and GQDs-02 (right) samples.

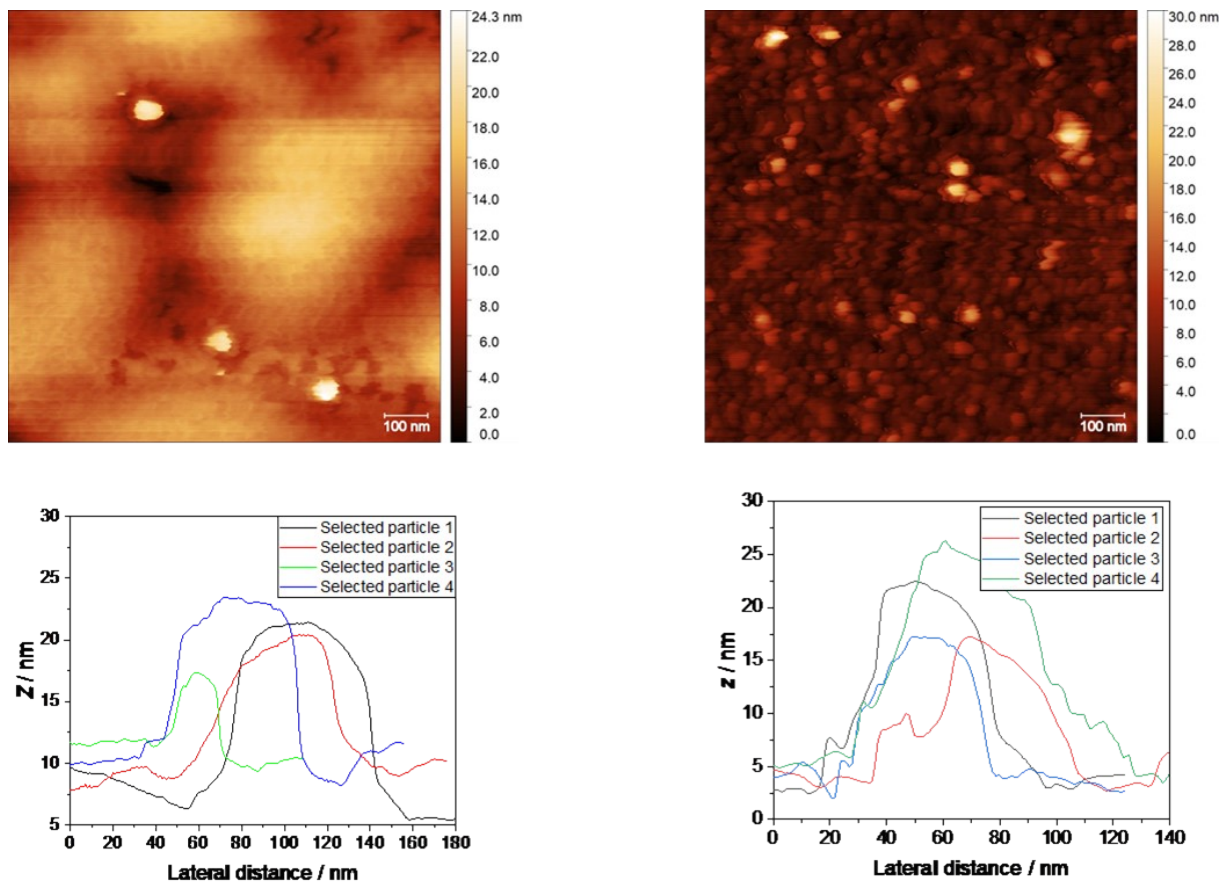


Fig. S5. AFM images (up) and height profiles (down) of GQDs-01 (left) and GQDs-02 (right) samples. Note that due to the limitation of the resolution of the tip, the lateral size might not be reliable.

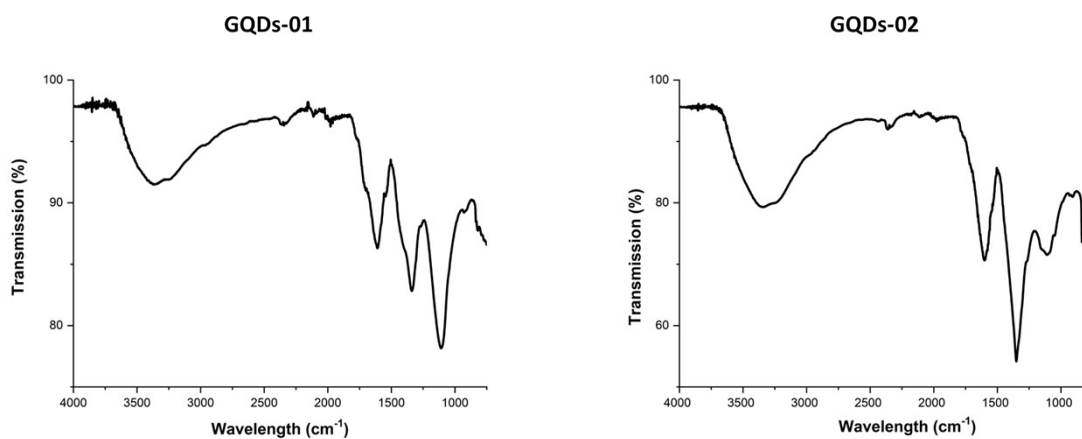


Fig. S6. FTIR pattern of GQDs-01 (left) and GQDs-02 (right) samples.

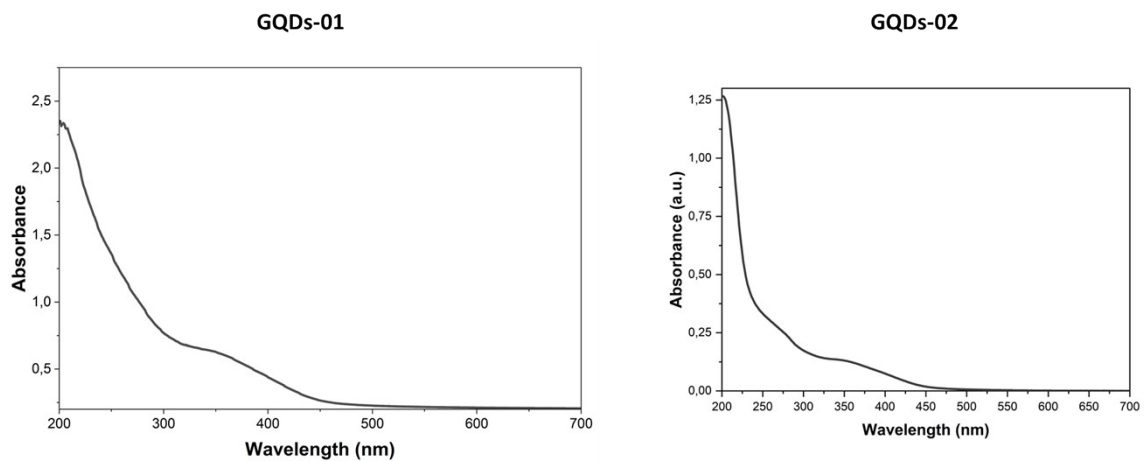


Fig. S7. UV-vis spectra of GQDs-01 (left) and GQDs-02 (right) samples.

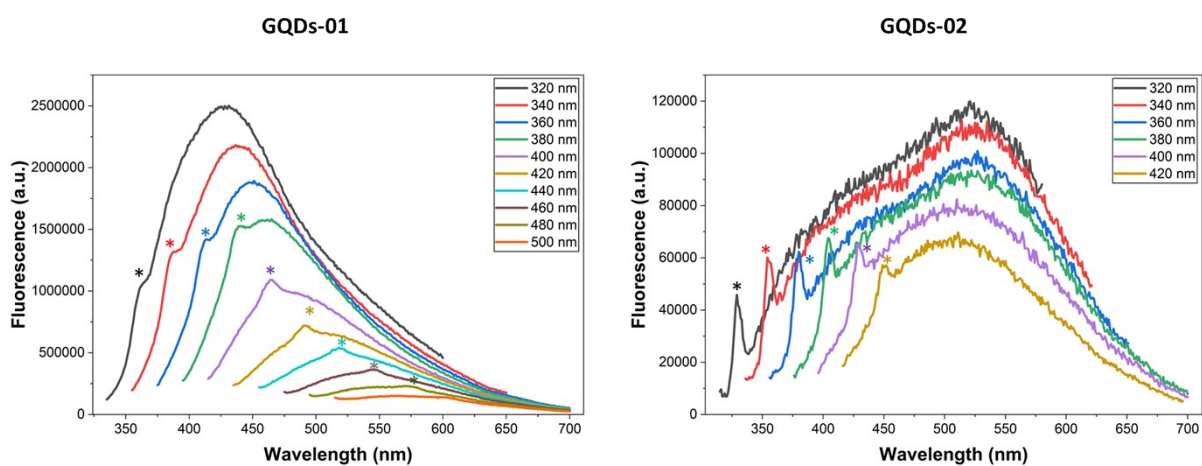


Fig. S8. PL spectra of aqueous solution of GQDs-01 (left) and GQDs-02 (right) samples (20 μ g/mL) at diverse excitation wavelengths. Peaks marked with an asterisk (*) originate from Raman scattering of water (O–H vibrational modes), appearing at a fixed Raman shift relative to the excitation wavelength.